Generation of Entanglement from Mechanical Rotation

Marko Toroš,[1] Marion Cromb,[1] Mauro Paternostro,[2] and Daniele Faccio[1]
[1]School of Physics and Astronomy, University of Glasgow, Glasgow G12 8QQ, United Kingdom
[2]Centre for Quantum Materials and Technologies, School of Mathematics and Physics, Queen's University, Belfast BT7 1NN, United Kingdom

(Received 25 July 2022; revised 1 October 2022; accepted 24 October 2022; published 21 December 2022)

Many phenomena and fundamental predictions, ranging from Hawking radiation to the early evolution of the Universe rely on the interplay between quantum mechanics and gravity or more generally, quantum mechanics in curved spacetimes. However, our understanding is hindered by the lack of experiments that actually allow us to probe quantum mechanics in curved spacetime in a repeatable and accessible way. Here we propose an experimental scheme for a photon that is prepared in a path superposition state across two rotating Sagnac interferometers that have different diameters and thus represent a superposition of two different spacetimes. We predict the generation of genuine entanglement even at low rotation frequencies and show how these effects could be observed even due to the Earth's rotation. These predictions provide an accessible platform in which to study the role of the underlying spacetime in the generation of entanglement.

DOI: 10.1103/PhysRevLett.129.260401

Introduction.—Our understanding of the physical world rests on two theories constructed at the beginning of the 20th century. Quantum mechanics arose out of the necessity to explain new results coming from deceitfully simple experiments [1], while general relativity emerged by recognizing the profound equivalence between inertial and gravitational effects [2]. Yet, despite their numerous successes, we have little experimental evidence about the regime where the two theories meet. On the one hand, quantum mechanics is well tested in the domain of elementary particles up to the scale of atoms and macromolecules [3], while, on the other hand, the experimental evidence for gravitational effects is mostly limited to much larger length scales [4].

Nonetheless, over the decades a handful of experiments began testing quantum systems in the underlying spacetime. Among the most notable are the seminal works on neutron interferometry in the Earth's gravitational field [5,6]. These have led to a series of experiments which probe interference phenomena in the regime of Newtonian gravity [7–10] as well as to Sagnac interferometers probing noninertial rotational motion [11,12].

More recently, the development of photonic technologies have enabled the exploration of entanglement and multimode interference at the quantum-gravity interface. It has been shown that linear accelerations do not affect two-photon entanglement [13], while low-frequency rotations can modify two-photon Hong-Ou-Mandel interference [14], and that the antibunching signature of entanglement can be concealed or revealed by low-frequency rotations [15,16]. These initial works suggested general relativistic adaptations [14] to satellite-based missions [17] with new generalizations under development [18–22].

Ring laser gyroscopes have also achieved exquiste sensitivities in underground facilities [23], with proposals for testing the Lense-Thirring effect [24] and for constraining theories of gravity [25], offering an alernative to orbiting cryogenic gyroscopes [26] and to satellite laser ranging [27]. Moreover, Sagnac-based interferometers have been suggested for detecting gravitational waves from intermediate-mass black hole mergers [28], and are the backbone of fundamental and technological applications [29,30].

The above experiments and proposals, striking in their own right, have in common that the degree of entanglement remains unaltered by the underlying spacetime. Although theoretical calculations are indicating that entanglement is not an invariant quantity in a general relativistic setting [31,32] any variations become vanishingly small at low accelerations or in weak gravity [13]. All experimental and theoretical results are thus suggesting, at least in the regime within reach of typical laboratory experiments, that entanglement remains unaltered by the underlying spacetime.

As we show here, this is not the case: we provide a protocol for *generating entanglement* in the regime of low accelerations. We exploit a previously unexplored coupling that arises in noninertial rotating reference frames. We will

focus on an implementation with photonic systems, which offers the prospect of an experimental implementation using the path-polarization degrees of freedom. In particular, we will show that an initially separable state becomes *maximally entangled* even at low-frequency of rotations $\sim$1 Hz, using fibers of length $\sim$30 m, and a platform of radius $\sim$0.5 m. The scheme relies on a single photon source, the original use of a dual-Sagnac interferometer —which allows for the interpretation of our results in terms of spacetime superpositions—and protocols for witnessing quantum entanglement. We discuss the implications for the quantum-gravity interface, and conclude by estimating the experimental requirements to test the generation of entanglement driven by the Earth's daily rotation.

Coupling rotations and paths.—The study of rotating reference frames has led to major breakthroughs in experimental and theoretical physics, from Sagnac's test of special relativity [33,34], to Einstein's general theory of relativity [35]. In this Letter, we are interested in dynamical effects that arise from the motion of quantum systems in a rotating Minkowski spacetime.

The equations of motion can be constructed from two simple observations. First, noninertial rotational effects scale with the frequency of rotation $\mathbf{\Omega}$. Second, from the viewpoint of the corotating observer, free-moving objects are rotating around the origin, and must thus possess an angular momentum $\boldsymbol{J}$. We are thus led to the Hamiltonian term $\sim\mathbf{\Omega}\cdot\boldsymbol{J}$ [36]. The situation further simplifies for motion on a circle with the axis of rotation located at the origin of the coordinates [15]

$$H_{\mathrm{rot}} = H + \Omega r p, \tag{1}$$

where H is the usual Hamiltonian that is present already in an inertial reference frame, and r (p) is the radial position (tangential momentum) of the system.

Let us now consider the motion of photons in such a rotating spacetime. We can gain an intuitive understanding of Eq. (1) by recalling the relation between energy and momentum [37,38], $p = \pm H/(nc)$, where n is the refractive index of the medium, and c is the speed of light. The Hamiltonian hence transforms to $H^{(\pm)}_{\mathrm{rot}} = H(1 \pm [\Omega r/nc])$, where $\pm(\Omega r/nc)$ can be seen as the Doppler shift of the energy due to the rotational motion (with the sign indicating counterrotating or corotating motion with respect to the platform). It is precisely this imbalance between the two directions of motion that is responsible for the Sagnac phase, $\phi_s = (H^{(+)}_{\mathrm{rot}} - H^{(-)}_{\mathrm{rot}})t/\hbar = 2H\Omega r t/(\hbar nc)$, where t is the time of flight. In particular, setting $H = \hbar\omega$ and $t = 2\pi r/(c/n)$, we then readily find the usual expression for the Sagnac phase [39–41]

$$\phi_s = \frac{4\Omega\omega\mathcal{A}_s}{c^2}, \tag{2}$$

where ω is the optical frequency, and $\mathcal{A}_s = \pi r^2$ denotes area enclosed by the interferometer.

The term $\Omega r p$ in Eq. (1) can be also viewed as a *coupling* between the position, r, and the momentum, p, with the values depending on the path followed by the photon. In a nonrotating reference frame $\Omega = 0$ and the coupling vanishes. As we will see, this coupling can be exploited to entangle the path-polarization degrees of freedom of photons.

Experimental scheme.—The experimental setup is shown in Fig. 1(a). We consider the initial state

$$|\psi_{\mathrm{initial}}\rangle = \frac{1}{2}(|a\rangle + |b\rangle)(|H\rangle + |V\rangle), \tag{3}$$

where a, b denote the path, and H, V denote the polarization (cf. Sec. A of the Supplemental Material [42] and Ref. [43] for more details). We note that the initial state is separable into a path part, $(|a\rangle + |b\rangle)/\sqrt{2}$, and a polarization part $(|H\rangle + |V\rangle)/\sqrt{2}$.

We then send the photon into *four* different paths with different radii and momenta, namely (r_a, p), $(r_a, -p)$, (r_b, p), and $(r_b, -p)$. As a consequence, the noninertial rotational motion, via the coupling $\Omega r p$ in Eq. (1), induces four different phases in $|\psi_{\mathrm{initial}}\rangle$. In particular, we find the final state

$$\begin{aligned}|\psi_{\mathrm{final}}\rangle = \frac{1}{2}(&|a\rangle[e^{-\frac{i\Omega r_a pt}{\hbar}}|H\rangle + e^{\frac{i\Omega r_a pt}{\hbar}}|V\rangle] \\ &+ |b\rangle[e^{-\frac{i\Omega r_b pt}{\hbar}}|H\rangle + e^{\frac{i\Omega r_b pt}{\hbar}}|V\rangle]),\end{aligned} \tag{4}$$

where $t = nl/c$ is the flight time with n the refractive index of the fiber, l the length of the fibers (assumed equal for the two paths), c the speed of light, $p = E/(nc) = \hbar\omega/(nc)$ the momentum, and ω the photon frequency. We note that the phases can be rewritten as

$$\phi_j \equiv \frac{\Omega r_j p t}{\hbar} = \frac{\Omega\omega\mathcal{A}_j}{c^2}, \quad (j = a, b), \tag{5}$$

where $\mathcal{A}_j = r_j l$ is an effective area of the loop. The phases ϕ_j can thus be seen as variants of the Sagnac phase introduced in Eq. (2). Importantly, such phases do not depend on the refractive index of the medium, indicating that the effect highlighted here does not stem from light-matter coupling in the fibers but rather that it is rooted in relativity [39–41].

Let us consider first the case $\Omega = 0$. We note that the final state in Eq. (4) reduces to the initial state in Eq. (3) and thus a nonrotating platform has no effect on entanglement, as expected. Conversely when $\Omega \neq 0$ the state in Eq. (4) will, in general, become entangled (as we can no longer write it as the product of the path and polarization states). The effect of mechanical rotation is to rotate the polarization state depending on the photon path a, b—as we will see the polarization states in Eq. (4) associated to paths a and b can become orthogonal (the overall polarization states in the square brackets), resulting in a maximally

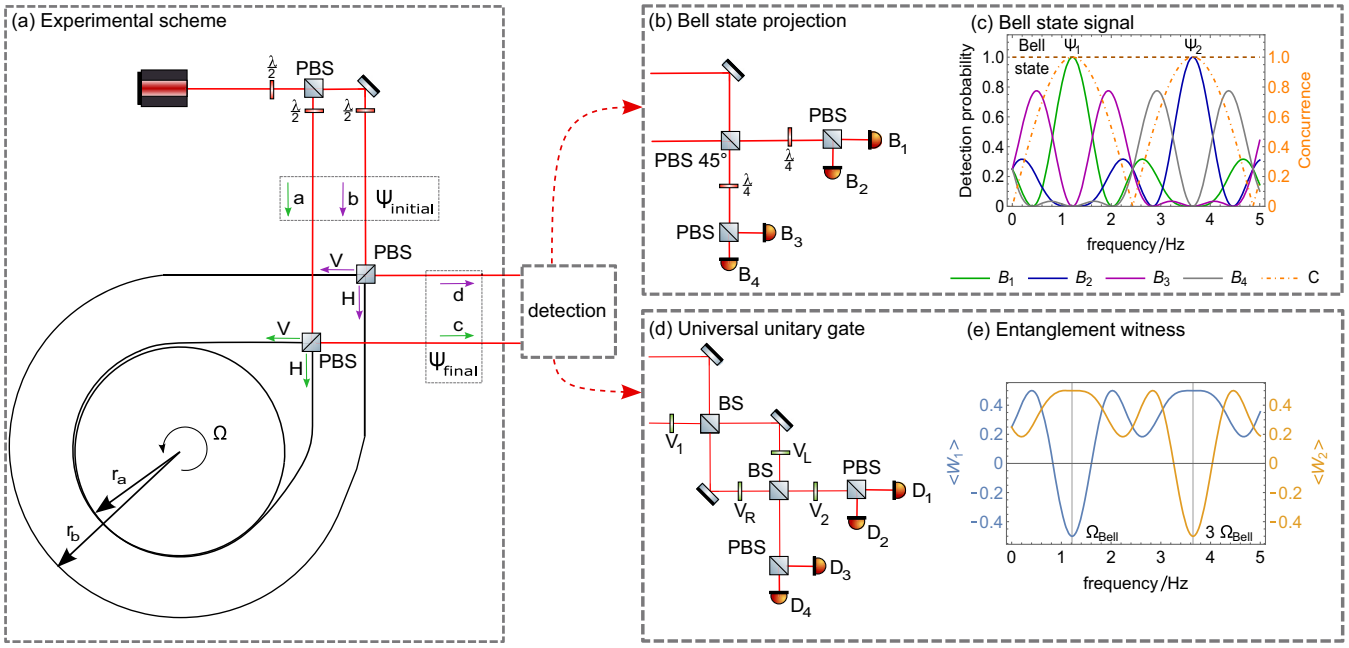

FIG. 1. Scheme for generating path-polarization entanglement from mechanical rotation. (a) The scheme consists of a single photon source, polarizing beam splitters (PBSs), and half-wave plates (HWPs) denoted by $\lambda/2$. We consider fiber loops with radii $r_b \sim 0.5$ m, $r_a \sim r_b/2$ (with total length $l \sim 2\pi r_b N_b$ with winding number $N_b = 10$) and a photon wavelength 800 nm. The experimental setup is placed on a platform which can be set in rotation with frequency Ω. The green and purple arrows indicate the paths a, b, while the polarization is denoted by H, V. We start with a separable path-polarization photon $|\psi_{\text{initial}}\rangle$; depending on the frequency of rotation Ω the final photon $|\psi_{\text{final}}\rangle$ can remain separable or becomes entangled. We can generate a maximally entangled Bell state by tuning the frequency of the platform to $\Omega_{\text{Bell}} = \pi c^2/(2\omega\mathcal{A})$, where ω is the mean photon frequency, and $\mathcal{A} = \Delta r l$ is the effective area of the interferometer ($\Delta r = r_b - r_a$ is the difference of the radii, and l is the path length assumed to be equal for the a, b paths). (b) The detector B_j measures the Bell state ψ_j ($j = 1, \ldots, 4$). The first PBS is rotated by $\pi/4$, and the quarter-wave plates (QWPs) are denoted by $\lambda/4$ (with the fast axis oriented at $\pi/4$ which transforms circular polarization to linear polarization). (c) The detector $B1$ ($B2$) measures the maximally entangled Bell state $\psi_1(\psi_2)$ at frequency $\Omega_{\text{Bell}}(3\Omega_{\text{Bell}})$, where the concurrence achieves the maximum possible value $C = 1$. We find $\Omega_{\text{Bell}} \sim 2\pi \times 1.2$ Hz, which can be readily achieved with similar photonic setups [14]. (d) Universal unitary gate for single-photon two-qubit states which can be used for tomographic reconstruction or implementing entanglement witnesses. The two beam splitters (BSs) together with the mirrors form a Mach-Zehnder interferometer, and $V_j (j = 1, R, L, 2)$ denotes an optical element composed of a HWP, two enclosing QWPs, and a phase shifter. (e) Optimal entanglement witnesses $\mathcal{W}_1$ ($\mathcal{W}_2$) for the maximally entangled Bell state $\psi_1(\psi_2)$ as a function of rotation frequency. Entanglement is witnessed when $\mathcal{W}_j < 0$ ($j = 1, 2$).

entangled path-polarization state. This shows that noninertial rotating motion generates entanglement.

Spacetime superpositions.—The presented mechanism for the generation of entanglement, arising from the ostensibly relativistic Sagnac effect [39–41], poses fundamental questions about the role of the underlying spacetime. Although the final state in Eq. (4) can be derived within the framework of quantum field theory in curved spacetime, the two rotating Sagnac interferometers shown in Fig. 1 are suggestive of an interpretation in terms of spacetime superpositions. This can be put in a mathematical form by modeling the spacetimes inside the two fiber loops. The metric is given by [15]

$$ds_j^2 = c^2(1 - \Omega^2 r_j^2/c^2)dt^2 - 2\Omega r_j^2 dt d\phi - r_j^2 d\phi^2, \quad (j = a, b), \tag{6}$$

where the time t and polar angle ϕ are the two coordinates, and the subscripts a (b) denote the small (big) fiber loop. The $1+1$ metric in Eq. (6) is fully specified by two quantities: the angular frequency of rotation Ω and the radius r_j. Together, they encode the specific relative angular momentum Ωr_j^2 in the $dtd\phi$ term, and the factor $\Omega^2 r_j^2/c^2$, responsible for time dilation, in the dt^2 term [44,45]. To account for these two effects, which are properties of the spacetime and not of the photons, we introduce the states $|r_j, \Omega\rangle$ ($j = a, b$).

As the photon enters the two fiber loops we are thus led to consider the following joint photon-spacetime state

$$|\psi\rangle = \frac{1}{2}(|a\rangle|r_a, \Omega\rangle + |b\rangle|r_b, \Omega\rangle)(|p\rangle|H\rangle + |-p\rangle|V\rangle), \tag{7}$$

where $|r_j, \Omega\rangle$ ($j = a, b$) denotes the state associated to the metric in Eq. (6), and $|\pm p\rangle$ is the photon momentum state.

The state $|a\rangle|H\rangle$ appearing in Eqs. (3) and (4) can be thus seen as a shorthand notation for the photon-spacetime state $|a\rangle|r_a,\Omega\rangle|p\rangle|H\rangle$ (and similarly for the other three states $|a\rangle|V\rangle$, $|b\rangle|H\rangle$, and $|b\rangle|V\rangle$).

In particular, the term $|a\rangle|r_a,\Omega\rangle + |b\rangle|r_b,\Omega\rangle$ in Eq. (7) can be interpreted as a superposition of spacetimes associated with the two Sagnac interferometers. The state of the metric $|r_j,\Omega\rangle$ ($j = a, b$) will induce phases proportional to $r_j\Omega$, which is a key ingredient in entangling the path-polarization degrees of freedom of the photon. Hence, by promoting the metric in Eq. (6) to a quantum state we have shown that the generation of entanglement can be linked to the concept reminiscent of quantum reference frames [46,47].

Maximizing entanglement.—The state in Eq. (4) will become maximally entangled when the overall polarization states in the square brackets of Eq. (4) become orthogonal. This is achieved when the overlap S between such states reduces to zero. Using the orthonormality of the $|H\rangle$, $|V\rangle$ polarization states, we find

$$\begin{aligned} S &= \frac{1}{2}[e^{i\phi_a}\langle H| + e^{-i\phi_a}\langle V|][e^{-i\phi_b}|H\rangle + e^{i\phi_b}|V\rangle] \\ &= \cos(\Omega\omega\Delta r l/c^2), \end{aligned} \tag{8}$$

where we have set $pt/\hbar = \omega l/c^2$ ($\Delta r = r_b - r_a$ is the difference of the radii, and l is the path length assumed to be equal for the a, b paths). We thus have $S = 0$ (and the path-polarization state becomes maximally entangled) when the rotation frequency Ω takes the values

$$\Omega_{\text{Bell}} \equiv \frac{(2k+1)\pi c^2}{2\omega\mathcal{A}}, \quad (k \in \mathbb{Z}), \tag{9}$$

where $\mathcal{A} = \Delta r l$ is the effective area of the interferometer. If we set the rotation frequency Ω to any odd frequency multiple of Ω_{Bell} we will also generate a maximally entangled Bell state, while if we tune Ω to any even frequency multiple of Ω_{Bell}, the state remains separable. We find the Bell states

$$|\psi_1\rangle = \frac{1}{2}(|a\rangle[e^{-i\frac{\pi r_a}{2\Delta r}}|H\rangle + e^{i\frac{\pi r_a}{2\Delta r}}|V\rangle] + |b\rangle[e^{-i\frac{\pi r_b}{2\Delta r}}|H\rangle + e^{i\frac{\pi r_b}{2\Delta r}}|V\rangle]) \tag{10}$$

at $\Omega/\Omega_{\text{Bell}} = \ldots, -7, -3, 1, 5, \ldots$, and

$$\begin{aligned} |\psi_2\rangle = \frac{1}{2}(&|a\rangle[e^{-i\frac{3\pi r_a}{2\Delta r}}|H\rangle + e^{i\frac{3\pi r_a}{2\Delta r}}|V\rangle] \\ &+ |b\rangle[e^{-i\frac{3\pi r_b}{2\Delta r}}|H\rangle + e^{i\frac{3\pi r_b}{2\Delta r}}|V\rangle]) \end{aligned} \tag{11}$$

at $\Omega/\Omega_{\text{Bell}} = \ldots, -5, -1, 3, 7\ldots$. Noninertial rotational motion is thus able to generate two distinct Bell states $|\psi_1\rangle$,$|\psi_2\rangle$—from an initially separable state—solely by tuning the frequency of rotation.

Verifying entanglement.—We can verify the generation of maximal entanglement using the Bell state projection scheme [48] shown in Fig. 1(b) with the experimental signature in Fig. 1(c). In particular, we compute the concurrence $C = 2|\mathfrak{a}_1\mathfrak{a}_4 - \mathfrak{a}_2\mathfrak{a}_3|$ as witness of the degree of entanglement for different rotation frequencies [49], where $\mathfrak{a}_1, \ldots, \mathfrak{a}_4$ denote the four phase factors (including the numerical prefactor $1/2$) in the order appearing in Eq. (4). When the probability of detection in B_1 or B_2 is unity then the concurrence reaches the value $C = 1$, indicating maximum entanglement (see Supplemental Material B and C for more details [42]).

We can also use the universal unitary gate for single-photon two-qubit states [50] shown in Fig. 1(d) to perform a full tomographic reconstruction or to implement a fidelity-based optimal entanglement witness [51]. The entanglement established in the system is validated whenever the entanglement witness $\mathcal{W}_1$ or $\mathcal{W}_2$ shown in Fig. 1(e) acquires a negative value (see Supplemental Material D and E for more details [42]). In Sec. F of the Supplemental Material [42], we also propose an alternative experimental scheme, based on a single-loop configuration, that is capable of achieving similar results to those reported here, but is not susceptible to alignment imperfections between the two loops (see Sec. G of Supplemental Material [42] for a robustness analysis).

Discussion.—We have shown that path-polarization entanglement can no longer be viewed as an invariant quantity, but rather requires us to view it as a dynamical quantity that can be completely altered already by low-frequency rotations.

The literature sometimes makes a distinction between path-polarization entanglement and multiphoton entanglement. However, one can transfer intraphoton entanglement of the two separable photons to a two-photon entangled state using known entanglement swapping protocols resulting in a polarization-entangled photon pair [52,53]. The scheme of Fig. 1 could be thus combined with entanglement swapping protocols to generate multiphoton entanglement, offering an intriguing alternative to electrodynamic protocols [54–56].

The developed scheme is also not a peculiarity of photonic systems or rotations, but readily offers the possibility of adaptations and generalizations. It can be adapted to matter-wave interferometers, as the Hamiltonian in Eq. (1) applies to any system, whether massless or massive. The scheme could also be modified to probe other gravitational couplings, such as those involving linear accelerations and spacetime curvature, although such effects are typically weaker [57] and would require a dedicated space mission [17]. Here we have focused on the strongest effect that emerges directly in a rotating reference frame in a Minkowski spacetime. The proposed scheme is thus also fundamentally different from gravitationally induced entanglement between two massive

systems [58,59], which will test the quantum nature of perturbations around the Minkowski spacetime [60–63].

Other tests of the quantum-gravity interface aim to probe specific quantum gravity phenomena [64] such as holographic fluctuations in spacetime with Michelson interferometers [65–67], modified commutation relations with optomechanical setups [68], and energy dispersion in astronomical observations [69]. There are also a number of experiments which are testing for possible violations of Lorentz invariance [70] which could arise in certain models of quantum gravity [71], and there is ongoing effort to test the Penrose wave function collapse [72–74] as well as other nonstandard mechanisms of gravitational decoherence [75].

In summary, the scheme presented in this Letter addressed a hitherto unexplored process for the dynamical generation of entanglement from the underlying spacetime, which lends itself to a suggestive interpretation in terms of spacetime superpositions. Its core strength is that the predictions do not depend on specific models of quantum gravity but only on elementary notions of quantum field theory in curved spacetime. Furthermore, it is based on well-established tools from quantum optics, and it can be readily experimentally implemented using rotational frequency $\sim$1 Hz, fibers of length $\sim$30 m, and a platform of radius $\sim$0.5 m, similar to the numbers achieved in Ref. [14].

Even more intriguing is the fact that any rotation, even the Earth's daily one, may be used to continuously generate entanglement. Setting $\Omega_{\mathrm{Bell}} \sim \Omega_{\mathrm{Earth}} \sim 7 \times 10^{-5}$ Hz in Eq. (9) we find that the area required to generate maximal entanglement is about $\sim$0.65 km^2, which is comparable to the interferometer built by Michelson in 1925 [76,77]. It thus appears that testing the generation of entanglement sourced by the Earth's daily rotation is well within the domain of current experimental capabilities.

The authors acknowledge financial support from the Leverhulme Trust (Grants No. RPG-2020-197 and No. RPG-2018-266), the European Union's Horizon 2020 FET-Open project TEQ (766900), the Horizon Europe EIC-Pathfinder project QuCoM (101046973), the Royal Society Wolfson Fellowship (RSWF/R3/183013), the UK EPSRC (Grants No. EP/T028424/1, No. EP/T00097X/1, No. EP/W007444/1, No. EP/R030413/1, No. EP/M01326X/1, No. EP/R030081/1), the Department for the Economy Northern Ireland under the US-Ireland R&D Partnership Programme, and the Royal Academy of Engineering Chair in Emerging Technologies programme.

[1] Abraham Pais, *Inward Bound: Of Matter and Forces in the Physical World* (Clarendon Press, Oxford, New York, 1986).

[2] Abraham Pais and Stanley Goldberg, *"Subtle is the Lord…": The Science and the Life of Albert Einstein* (Oxford University Press, Oxford, UK, 1984).

[3] Yaakov Y. Fein, Philipp Geyer, Patrick Zwick, Filip Kiałka, Sebastian Pedalino, Marcel Mayor, Stefan Gerlich, and Markus Arndt, Quantum superposition of molecules beyond 25 kDa, Nat. Phys. **15**, 1242 (2019).

[4] Clifford M. Will, The confrontation between general relativity and experiment, Living Rev. Relativity **17**, 4 (2014).

[5] Roberto Colella, Albert W. Overhauser, and Samuel A. Werner, Observation of Gravitationally Induced Quantum Interference, Phys. Rev. Lett. **34**, 1472 (1975).

[6] S. A. Werner, J.-L. Staudenmann, and R. Colella, Effect of Earth's Rotation on the Quantum Mechanical Phase of the Neutron, Phys. Rev. Lett. **42**, 1103 (1979).

[7] Valery V. Nesvizhevsky, Hans G. Börner, Alexander K. Petukhov, Hartmut Abele, Stefan Baeßler, Frank J. Rueß, Thilo Stöferle, Alexander Westphal, Alexei M. Gagarski, Guennady A. Petrov, and Alexander V. Strelkov, Quantum states of neutrons in the Earth's gravitational field, Nature (London) **415**, 297 (2002).

[8] Jeffrey B. Fixler, G. T. Foster, J. M. McGuirk, and M. A. Kasevich, Atom interferometer measurement of the newtonian constant of gravity, Science **315**, 74 (2007).

[9] Peter Asenbaum, Chris Overstreet, Tim Kovachy, Daniel D. Brown, Jason M. Hogan, and Mark A. Kasevich, Phase Shift in an Atom Interferometer due to Spacetime Curvature across its Wave Function, Phys. Rev. Lett. **118**, 183602 (2017).

[10] Chris Overstreet, Peter Asenbaum, Joseph Curti, Minjeong Kim, and Mark A. Kasevich, Observation of a gravitational Aharonov-Bohm effect, Science **375**, 226 (2022).

[11] Brynle Barrett, Rémy Geiger, Indranil Dutta, Matthieu Meunier, Benjamin Canuel, Alexandre Gauguet, Philippe Bouyer, and Arnaud Landragin, The Sagnac effect: 20 years of development in matter-wave interferometry, C. R. Phys. **15**, 875 (2014).

[12] Guillaume Bertocchi, Olivier Alibart, Daniel Barry Ostrowsky, Sébastien Tanzilli, and Pascal Baldi, Single-photon Sagnac interferometer, J. Phys. B **39**, 1011 (2006).

[13] Matthias Fink, Ana Rodriguez-Aramendia, Johannes Handsteiner, Abdul Ziarkash, Fabian Steinlechner, Thomas Scheidl, Ivette Fuentes, Jacques Pienaar, Timothy C. Ralph, and Rupert Ursin, Experimental test of photonic entanglement in accelerated reference frames, Nat. Commun. **8**, 1 (2017).

[14] Sara Restuccia, Marko Toroš, Graham M. Gibson, Hendrik Ulbricht, Daniele Faccio, and Miles J. Padgett, Photon Bunching in a Rotating Reference Frame, Phys. Rev. Lett. **123**, 110401 (2019).

[15] Marko Toroš, Sara Restuccia, Graham M. Gibson, Marion Cromb, Hendrik Ulbricht, Miles Padgett, and Daniele Faccio, Revealing and concealing entanglement with non-inertial motion, Phys. Rev. A **101**, 043837 (2020).

[16] Marion Cromb, Sara Restuccia, Graham M. Gibson, Marko Toros, Miles J. Padgett, and Daniele Faccio, Controlling photon entanglement with mechanical rotation, arXiv:2210.05628.

[17] Juan Yin, Yuan Cao, Yu-Huai Li, Sheng-Kai Liao, Liang Zhang, Ji-Gang Ren, Wen-Qi Cai, Wei-Yue Liu, Bo Li, Hui Dai *et al.*, Satellite-based entanglement distribution over 1200 kilometers, Science **356**, 1140 (2017).
[18] Marco Rivera-Tapia, Marcel I. Yáñez Reyes, A. Delgado, and G. Rubilar, Outperforming classical estimation of post-Newtonian parameters of Earth's gravitational field using quantum metrology, arXiv:2101.12126.
[19] Anthony J. Brady and Stav Haldar, Frame dragging and the Hong-Ou-Mandel dip: Gravitational effects in multiphoton interference, Phys. Rev. Res. **3**, 023024 (2021).
[20] Sebastian P. Kish and Timothy C. Ralph, Quantum effects in rotating reference frames, AVS Quantum Sci. **4**, 011401 (2022).
[21] Roy Barzel, David Edward Bruschi, Andreas W. Schell, and Claus Lämmerzahl, Observer dependence of photon bunching: The influence of the relativistic redshift on Hong-Ou-Mandel interference, Phys. Rev. D **105**, 105016 (2022).
[22] Thomas Mieling, Christopher Hilweg, and Philip Walther, Measuring space-time curvature using maximally path-entangled quantum states, Phys. Rev. A **106**, L031701 (2022).
[23] Angela D. Di Virgilio, Carlo Altucci, Francesco Bajardi, Andrea Basti, Nicolò Beverini, Salvatore Capozziello, Giorgio Carelli, Donatella Ciampini, Francesco Fuso, Umberto Giacomelli *et al.*, Sensitivity limit investigation of a Sagnac gyroscope through linear regression analysis, Eur. Phys. J. C **81**, 1 (2021).
[24] Angela D. V. Di Virgilio, Jacopo Belfi, Wei-Tou Ni, Nicolo Beverini, Giorgio Carelli, Enrico Maccioni, and Alberto Porzio, Ginger: A feasibility study, Eur. Phys. J. Plus **132**, 157 (2017).
[25] Salvatore Capozziello, Carlo Altucci, Francesco Bajardi, Andrea Basti, Nicolò Beverini, Giorgio Carelli, Donatella Ciampini, Angela D. V. Di Virgilio, Francesco Fuso, Umberto Giacomelli *et al.*, Constraining theories of gravity by ginger experiment, Eur. Phys. J. Plus **136**, 1 (2021).
[26] C. W. F. Everitt, D. B. DeBra, B. W. Parkinson, J. P. Turneaure, J. W. Conklin, M. I. Heifetz, G. M. Keiser, A. S. Silbergleit, T. Holmes, J. Kolodziejczak *et al.*, Gravity Probe B: Final Results of a Space Experiment to Test General Relativity, Phys. Rev. Lett. **106**, 221101 (2011).
[27] Ignazio Ciufolini and Erricos C. Pavlis, A confirmation of the general relativistic prediction of the Lense-Thirring effect, Nature (London) **431**, 958 (2004).
[28] Sylvester Lacour, F. H. Vincent, M. Nowak, A. Le Tiec, V. Lapeyrere, L. David, P. Bourget, A. Kellerer, K. Jani, J. Martino *et al.*, SAGE: Finding IMBH in the black hole desert, Classical Quantum Gravity **36**, 195005 (2019).
[29] Heonoh Kim, Osung Kwon, and Han Seb Moon, Pulsed Sagnac source of polarization-entangled photon pairs in telecommunication band, Sci. Rep. **9**, 1 (2019).
[30] Youn Seok Lee, Mengyu Xie, Ramy Tannous, and Thomas Jennewein, Sagnac-type entangled photon source using only conventional polarization optics, Quantum Sci. Technol. **6**, 025004 (2021).
[31] Ivette Fuentes-Schuller and Robert B. Mann, Alice Falls into a Black Hole: Entanglement in Noninertial Frames, Phys. Rev. Lett. **95**, 120404 (2005).
[32] Paul M. Alsing and Ivette Fuentes, Observer-dependent entanglement, Classical Quantum Gravity **29**, 224001 (2012).
[33] Georges Sagnac, L'éther lumineux démontré par l'effet du vent relatif d'éther dans un interféromètre en rotation uniforme, C.R. Acad. Sci. **157**, 708 (1913).
[34] Georges Sagnac, Sur la preuve de la réalité de l'éther lumineux par l'expérience de l'interférographe tournant, C.R. Acad. Sci. **157**, 1410 (1913).
[35] Armin Hermann, Albert Einstein/Arnold Sommerfeld: Briefwechsel, Exchange of Letters between Albert Einstein and Arnold Sommerfeld (Basel and Stuttgart, Schwabe, Erikson, Erik, 1979).
[36] Jan Ivar Korsbakken and Jon Magne Leinaas, Fulling-Unruh effect in general stationary accelerated frames, Phys. Rev. D **70**, 084016 (2004).
[37] Miles J. Padgett, On diffraction within a dielectric medium as an example of the Minkowski formulation of optical momentum, Opt. Express **16**, 20864 (2008).
[38] Stephen M. Barnett, Resolution of the Abraham-Minkowski Dilemma, Phys. Rev. Lett. **104**, 070401 (2010).
[39] Evert Jan Post, Sagnac effect, Rev. Mod. Phys. **39**, 475 (1967).
[40] Ronald Anderson, H. R. Bilger, and G. E. Stedman, "Sagnac" effect: A century of earth-rotated interferometers, Am. J. Phys. **62**, 975 (1994).
[41] Grigorii B. Malykin, The Sagnac effect: Correct and incorrect explanations, Phys. Usp. **43**, 1229 (2000).
[42] See Supplemental Material at http://link.aps.org/supplemental/10.1103/PhysRevLett.129.260401 for A. Initial state preparation and basic definitions, B. Bell state basis, C. Bell state projection scheme, D. Construction of optimal entanglement witness, E. Measuring entanglement witnesses using the universal unitary gate, F. Alternative single loop scheme, G. Robustness estimates.
[43] Hans-A. Bachor and Timothy C. Ralph, *A Guide to Experiments in Quantum Optics* (John Wiley & Sons, New York, 2019).
[44] Kip S. Thorne, Charles W. Misner, and John Archibald Wheeler, *Gravitation* (Freeman, San Francisco, CA, 2000).
[45] David A. Vallado, *Fundamentals of Astrodynamics and Applications* (Springer Science & Business Media, New York, 2001), Vol. 12.
[46] Yakir Aharonov and Tirzah Kaufherr, Quantum frames of reference, Phys. Rev. D **30**, 368 (1984).
[47] Flaminia Giacomini, Esteban Castro-Ruiz, and Časlav Brukner, Relativistic Quantum Reference Frames: The Operational Meaning of Spin, Phys. Rev. Lett. **123**, 090404 (2019).
[48] Yoon-Ho Kim, Single-photon two-qubit entangled states: Preparation and measurement, Phys. Rev. A **67**, 040301 (2003).
[49] Scott Hill and William K. Wootters, Entanglement of a Pair of Quantum Bits, Phys. Rev. Lett. **78**, 5022 (1997).
[50] Berthold-Georg Englert, Christian Kurtsiefer, and Harald Weinfurter, Universal unitary gate for single-photon two-qubit states, Phys. Rev. A **63**, 032303 (2001).
[51] Otfried Gühne and Géza Tóth, Entanglement detection, Phys. Rep. **474**, 1 (2009).

[52] S. Adhikari, A. S. Majumdar, Dipankar Home, and A. K. Pan, Swapping path-spin intraparticle entanglement onto spin-spin interparticle entanglement, Europhys. Lett. **89**, 10005 (2010).
[53] Asmita Kumari, Abhishek Ghosh, Mohit Lal Bera, and A. K. Pan, Swapping intraphoton entanglement to interphoton entanglement using linear optical devices, Phys. Rev. A **99**, 032118 (2019).
[54] Zihao Chen, Yao Zhou, and Jung-Tsung Shen, Photon antibunching and bunching in a ring-resonator waveguide quantum electrodynamics system, Opt. Lett. **41**, 3313 (2016).
[55] Zihao Chen, Yao Zhou, and Jung-Tsung Shen, Dissipation-induced photonic-correlation transition in waveguide-QED systems, Phys. Rev. A **96**, 053805 (2017).
[56] Zihao Chen, Yao Zhou, Jung-Tsung Shen, Pei-Cheng Ku, and Duncan Steel, Two-photon controlled-phase gates enabled by photonic dimers, Phys. Rev. A **103**, 052610 (2021).
[57] Magdalena Zych, Fabio Costa, Igor Pikovski, Timothy C. Ralph, and Časlav Brukner, General relativistic effects in quantum interference of photons, Classical Quantum Gravity **29**, 224010 (2012).
[58] Sougato Bose, Anupam Mazumdar, Gavin W. Morley, Hendrik Ulbricht, Marko Toroš, Mauro Paternostro, Andrew A. Geraci, Peter F. Barker, M. S. Kim, and Gerard Milburn, Spin Entanglement Witness for Quantum Gravity, Phys. Rev. Lett. **119**, 240401 (2017).
[59] Chiara Marletto and Vlatko Vedral, Gravitationally Induced Entanglement between Two Massive Particles is Sufficient Evidence of Quantum Effects in Gravity, Phys. Rev. Lett. **119**, 240402 (2017).
[60] Ryan J. Marshman, Anupam Mazumdar, and Sougato Bose, Locality and entanglement in table-top testing of the quantum nature of linearized gravity, Phys. Rev. A **101**, 052110 (2020).
[61] Daine L. Danielson, Gautam Satishchandran, and Robert M. Wald, Gravitationally mediated entanglement: Newtonian field versus gravitons, Phys. Rev. D **105**, 086001 (2022).
[62] Sougato Bose, Anupam Mazumdar, Martine Schut, and Marko Toroš, Mechanism for the quantum natured gravitons to entangle masses, Phys. Rev. D **105**, 106028 (2022).
[63] Marios Christodoulou, Andrea Di Biagio, Markus Aspelmeyer, Časlav Brukner, Carlo Rovelli, and Richard Howl, Locally mediated entanglement through gravity from first principles, arXiv:2202.03368.
[64] Giovanni Amelino-Camelia, Quantum-spacetime phenomenology, Living Rev. Relativity **16**, 5 (2013).
[65] Aaron Chou, Henry Glass, H. Richard Gustafson, Craig J. Hogan, Brittany L. Kamai, Ohkyung Kwon, Robert Lanza, Lee McCuller, Stephan S. Meyer, Jonathan W. Richardson *et al.*, Interferometric constraints on quantum geometrical shear noise correlations, Classical Quantum Gravity **34**, 165005 (2017).
[66] Sander M. Vermeulen, Lorenzo Aiello, Aldo Ejlli, William L. Griffiths, Alasdair L. James, Katherine L. Dooley, and Hartmut Grote, An experiment for observing quantum gravity phenomena using twin table-top 3d interferometers, Classical Quantum Gravity **38**, 085008 (2021).
[67] Erik P. Verlinde and Kathryn M. Zurek, Observational signatures of quantum gravity in interferometers, Phys. Lett. B **822**, 136663 (2021).
[68] Igor Pikovski, Michael R. Vanner, Markus Aspelmeyer, M. S. Kim, and Časlav Brukner, Probing Planck-scale physics with quantum optics, Nat. Phys. **8**, 393 (2012).
[69] Giovanni Amelino-Camelia, John Ellis, N. E. Mavromatos, Dimitri V. Nanopoulos, and Subir Sarkar, Tests of quantum gravity from observations of γ-ray bursts, Nature (London) **393**, 763 (1998).
[70] V. Alan Kostelecký and Neil Russell, Data tables for Lorentz and *CPT* violation, Rev. Mod. Phys. **83**, 11 (2011).
[71] David Mattingly, Modern tests of Lorentz invariance, Living Rev. Relativity **8**, 5 (2005).
[72] Roger Penrose, On gravity's role in quantum state reduction, Gen. Relativ. Gravit. **28**, 581 (1996).
[73] Sandro Donadi, Kristian Piscicchia, Catalina Curceanu, Lajos Diósi, Matthias Laubenstein, and Angelo Bassi, Underground test of gravity-related wave function collapse, Nat. Phys. **17**, 74 (2021).
[74] I. J. Arnquist *et al.*, Search for Spontaneous Radiation from Wave Function Collapse in the Majorana Demonstrator, Phys. Rev. Lett. **129**, 080401 (2022).
[75] Angelo Bassi, André Großardt, and Hendrik Ulbricht, Gravitational decoherence, Classical Quantum Gravity **34**, 193002 (2017).
[76] Albert Abraham Michelson, The effect of the Earth's rotation on the velocity of light, I., Astrophys. J. **61**, 137 (1925).
[77] Albert Abraham Michelson and Henry G. Gale, The effect of the Earth's rotation on the velocity of light, II., Astrophys. J. **61**, 140 (1925).